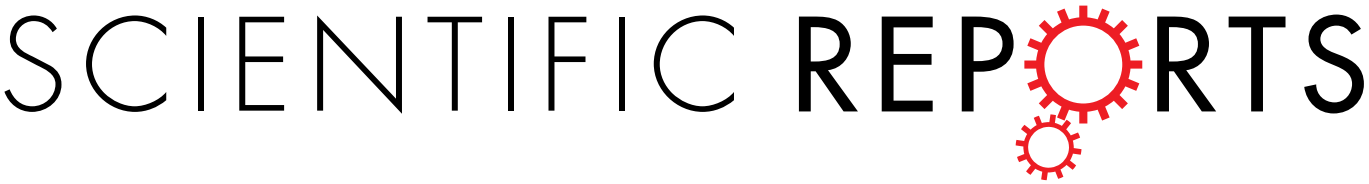

OPEN

Experimental realization of non-adiabatic universal quantum gates using geometric Landau-Zener-Stückelberg interferometry

Received: 01 October 2015
Accepted: 03 December 2015
Published: 07 January 2016

Li Wang[1], Tao Tu[1], Bo Gong[1], Cheng Zhou[2] & Guang-Can Guo[1]

High fidelity universal gates for quantum bits form an essential ingredient of quantum information processing. In particular, geometric gates have attracted attention because they have a higher intrinsic resistance to certain errors. However, their realization remains a challenge because of the need for complicated quantum control on a multi-level structure as well as meeting the adiabatic condition within a short decoherence time. Here, we demonstrate non-adiabatic quantum operations for a two-level system by applying a well-controlled geometric Landau-Zener-Stückelberg interferometry. By characterizing the gate quality, we also investigate the operation in the presence of realistic dephasing. Furthermore, the result provides an essential model suitable for understanding an interplay of geometric phase and Landau-Zener-Stückelberg process which are well explored separately.

In quantum information science, a primary goal is to implement precise universal gates, because they provide the fundamental building blocks for constructing complex operations[1]. A universal set of quantum logic gates requires two types of non-commutable operations or arbitrary rotations around two axes on the Bloch sphere of a quantum bit (qubit). For fault-tolerant quantum computation, it is believed that an infidelity or error threshold ranging between 10^{-4} and 10^{-2} is required[2–5]; however, most experimental implementations thus far have fallen short of these thresholds[6–11].

One promising approach towards this goal is to use quantum geometric phases which are acquired whenever a quantum system evolves cyclically along a path in the Hilbert space of quantum states[12–14]. In contrast to dynamical phases, geometric phases depend only on the geometry of the paths executed and are therefore resilient to certain types of errors[15–21], which offers a reliable method to improve the fidelity of the gate operations. In the original proposal on geometric quantum computation[22–26], if a system has multiple energy levels, a qubit is encoded in a doubly degenerate eigenspace. When the system evolves cyclically, it acquires not only a geometric phase factor but also undergoes a transition between the eigenstates in the degenerate subspace, which constitutes a set of universal unitary transformations for the qubit. In this technique, the system is typically changed adiabatically to guarantee the persistence of the degeneracy. However, the adiabatic condition makes any fast gate impossible, and consequently limits the application of the geometric gate operations in many quantum information tasks. A method for extending this process to non-adiabatic cases has been pursued[27–31]; however, the complex quantum control of the multi-level structure remains an experimental challenge.

In recent years, the Landau-Zener-Stückelberg (LZS) interference has become a powerful tool for studying two-level systems[11,32–35]. A new type of LZS interferometry has been proposed to have geometric fashion in a recent interesting letter[36], and an initial experiment is reported[37,38]. Inspired by this original proposal[39], here we joint the LZS interferometry and geometric quantum computation which are well explored separately in many quantum systems. We first outline the process in a general context[39] and then present an experimental realization in a semiconductor quantum dot architecture. The results demonstrate how harnessing a well-controlled geometric LZS interferometry builds quantum gates for a two-level system, which combines the advantages of

[1]Key Laboratory of Quantum Information, University of Science and Technology of China, Chinese Academy of Sciences, Hefei 230026, People's Republic of China. [2]Department of Physics and Astronomy, University of California at Los Angeles, California 90095, USA. Correspondence and requests for materials should be addressed to T.T. (email: tutao@ustc.edu.cn)

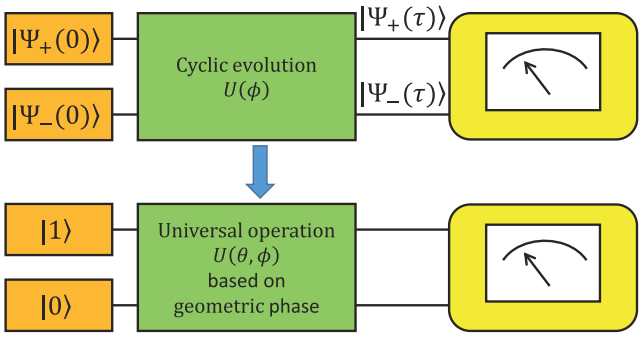

Figure 1. Quantum circuit for creation of cyclic evolution with a pair of orthogonal states $|\Psi_+(t)\rangle$ and $|\Psi_-(t)\rangle$, which is also equivalent to encoding the universal gate based on geometric phase in the computational basis states $|0\rangle$ and $|1\rangle$.

universality and speed. These types of geometric gates can thus be implemented conveniently in a wide variety of natural or artificial two-level systems.

Furthermore, in any realistic realization, a quantum system is influenced by its environment or control field leading to relaxation and dephasing during time evolution. The decoherence properties of geometric phase have been actively investigated in theory[15,40–47]. Therefore, there raises an interesting question about how an interplay of a geometric phase and a LZS dynamics manifests in the decoherence process. The present model can serve as a valuable tool to address this problem.

Results

Universal gates based on geometric phase for a two-level system. The principal idea is to generate a non-adiabatic, cyclic state evolution in a two-level system that results in a universal operation on the space spanned by the computational basis states, $|0\rangle$ and $|1\rangle$ (Fig. 1)[39]. Let us write a state at $t\,(0 \le t \le \tau)$ as $|\Psi(t)\rangle$. We consider a pair of orthogonal states $|\Psi_+(0)\rangle = \cos\frac{\theta}{2}|0\rangle + \sin\frac{\theta}{2}|1\rangle$ and $|\Psi_-(0)\rangle = -\sin\frac{\theta}{2}|0\rangle + \cos\frac{\theta}{2}|1\rangle$, which act as auxiliary states and evolve cyclically after the gate operation. Here θ is the spherical coordinate of the state vector on the Bloch sphere. During the cyclic evolution, a phase φ accumulates[13], and the evolution operator can be expressed as follows: $|\Psi_\pm(\tau)\rangle = \exp(\pm i\varphi)|\Psi_\pm(0)\rangle$ (see Supplementary Information for the definition of the phase factor during a cyclic evolution). Generally, this phase consists of both dynamical φ^d and geometric φ^g components. We note that in many schemes dynamical phase can also be acquired simultaneously in the cyclic evolution[15]. Specific operations or complex designs such as spin-echo technique can be used to remove the dynamical phase[15,39], and the total phase reduces to pure geometric fashion. Here we focus on an interplay of dynamical phase and geometric phase.

For an arbitrary input state $|\Psi_{\text{in}}(0)\rangle = a_+|\Psi_+(0)\rangle + a_-|\Psi_-(0)\rangle$, the final state is determined to be $|\Psi_{\text{out}}(\tau)\rangle = U_{(\tau,0)}|\Psi_{\text{in}}(0)\rangle$, and the matrix representation of the final operator that acts on the basis states $|0\rangle$ and $|1\rangle$ can be expressed as follows[39]:

$$U_{(\tau,0)} = \begin{pmatrix} \cos^2\frac{\theta}{2}\,e^{i\varphi} + \sin^2\frac{\theta}{2}\,e^{-i\varphi} & i\,\sin\,\theta\,\sin\,\varphi \\ i\,\sin\,\theta\,\sin\,\varphi & \sin^2\frac{\theta}{2}\,e^{i\varphi} + \cos^2\frac{\theta}{2}\,e^{-i\varphi} \end{pmatrix} \quad (1)$$

We can achieve a universal set of single qubit gates by selecting two non-commutable operations: $U(\theta_1,\ \varphi_1)$ and $U(\theta_2,\ \varphi_2)$.

Electron qubit in a double quantum dot. We describe an experiment conducted on an individual two-level system in a semiconductor electronic circuit (Fig. 2a, see Methods section for the details of devices and experimental techniques)[48,49]. An excess valence electron in the left and right quantum dots defines the charge occupation states $|0\rangle$ and $|1\rangle$. The charge qubit in a double quantum dot is typically regarded as a two-level system in the basis of $|0\rangle$ and $|1\rangle$. The Hamiltonian can be expressed as follows[48,50,51,52]:

$$H(t) = \varepsilon_0(t)|0\rangle\langle 0| + \varepsilon_1(t)|1\rangle\langle 1| + \Delta(|0\rangle\langle 1| + |1\rangle\langle 0|), \quad (2)$$

where ε_0 and ε_1 correspond to the discrete energy level in each dot; and Δ is the tunneling amplitude between the neighboring dots. In practice, the control pulse can be applied to vary the electrode voltages of the dots (for example, the left dot in our experiment), which leads to a change in the energy levels. The current approach is based on the cyclic evolution of the two orthogonal states $|\Psi_+(t)\rangle$ and $|\Psi_-(t)\rangle$, which are the instantaneous eigenstates of the system with energy eigenvalues $E_+(t) = \frac{1}{2} \pm \{\varepsilon_0(t) + \varepsilon_1 - \sqrt{[\varepsilon_0(t) - \varepsilon_1]^2 + 4\Delta^2}\}$ and $E_-(t) = \frac{1}{2}\{\varepsilon_0(t) + \varepsilon_1 + \sqrt{[\varepsilon_0(t) - \varepsilon_1]^2 + 4\Delta^2}\}$, respectively. For our experiments, the anti-crossing gap 2Δ is

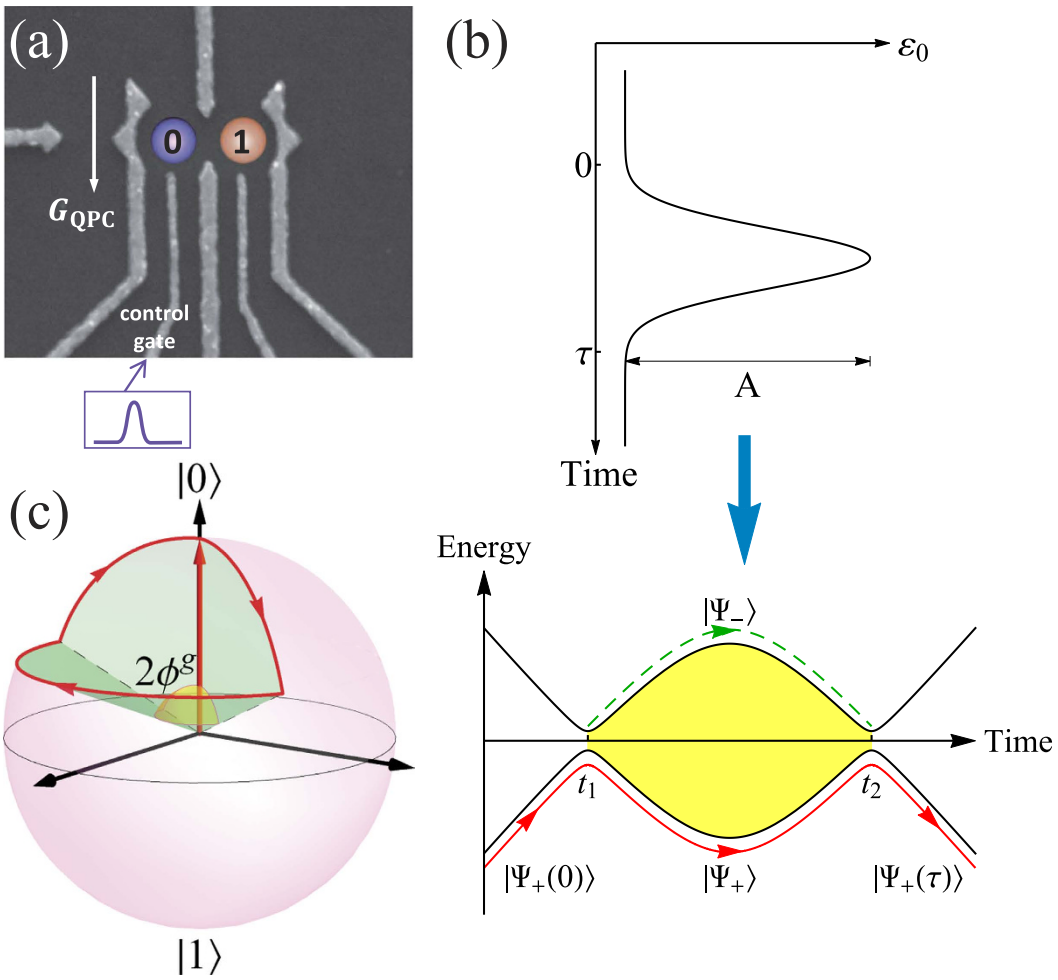

Figure 2. (**a**) Experimental setup for electron charge qubit in a double quantum dot. Scanning electron micrograph of the device that we used containing a double quantum dot and a nearby quantum point contact (QPC) sensor, with the locations of the states $|0\rangle$ and $|1\rangle$ indicated by circles. The electric control pulse profile is sketched in the down part of the electrode. (**b**) Top: Schematic illustration of the control pulse form. The driving pulse $\varepsilon_0(t)$ is implemented to vary the gate voltage of the dot and therefore the energy levels of the qubit. Down: The time evolution of the instantaneous energy levels. Driving the qubit from the initial state $|\Psi_+(0)\rangle$ through the avoided crossing induces Landau-Zener transitions between the two paths. The paths recombine and interfere when the qubit is brought back through the avoided crossing. For destructive interference, the system returns back to the initial state, i.e., a cyclic evolution for the state $|\Psi_+(\tau)\rangle = \exp(i\varphi)|\Psi_+(0)\rangle$. (**c**) Cyclic evolution represented on a Bloch sphere. The state space is the projected Hilbert space spanned by the basis states $|0\rangle$ and $|1\rangle$. The state vector fulfils the destructive interference condition and evolves cyclically under two Landau-Zener processes. The geometric phase φ^g is determined by half of the solid angle swept by the evolution loop.

fixed to 37.6 μeV and the reference level ε_1 is set to zero. In this system, known as charge qubit, the two-level system is affected by its electromagnetic environment. We have experimentally determined an energy relaxation time of $T_1 \approx 10$ ns and a phase coherence time of $T_2 \approx 3$ ns[48].

Realization of universal gates using geometric LZSM interferometry. Thus far, we have proposed a general method to achieve non-adiabatic universal quantum gates based on geometric phase accumulated by a two-level system. It is important to further consider implementing this technique with actual physical setups. This implementation can be achieved by driving the two-level system using a geometric LZS interferometry, with control parameters satisfying the condition of destructive interference.

The schematic diagram in Fig. 2b illustrates the energies of the instantaneous eigenstates of the qubit can be continuously tuned by the applied pulse $\varepsilon_0(t)$. The envelopes $\varepsilon_0(t)$ are Gaussian pulses with start point $\varepsilon_0(t)$, amplitude A and total pulse length of τ. As indicated in Fig. 2b, the energy levels have a minimum distance of anti-crossing, and this minimum distance is realized at times t_1 and t_2. In the first stage, the control pulse takes the system from the initial state $|\Psi_+(0)\rangle$ and passes through the anti-crossing point, at which a Landau-Zener transition occurs. The initial state is split into two occupied paths, one through $|\Psi_+(t)\rangle$ and the other through $|\Psi_-(t)\rangle$, which is analogous to an optical beam splitter[33,35]. In the second stage, the control pulse takes the system

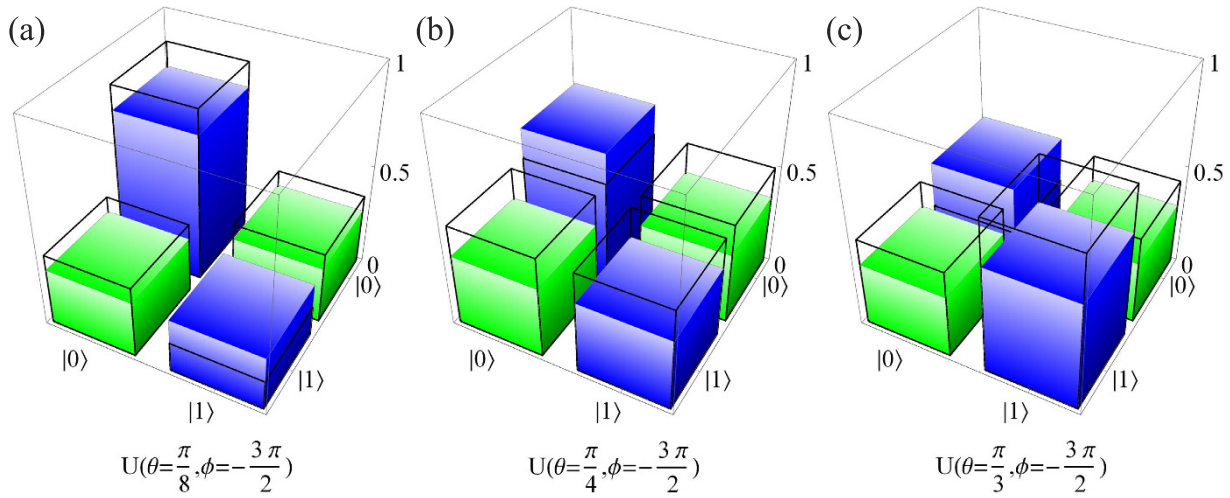

Figure 3. Characterization of the universal gates. Manhattan-style plots of the measured density matrices of the qubit states after the gate operations $U(\theta, \varphi)$: (**a**) $U\left(\theta = \frac{\pi}{8}, \varphi = -\frac{3\pi}{2}\right)$, (**b**) $U\left(\theta = \frac{\pi}{4}, \varphi = -\frac{3\pi}{2}\right)$, (**c**) $U\left(\theta = \frac{\pi}{3}, \varphi = -\frac{3\pi}{2}\right)$. The wire frames denote the theoretical values of ideal gates.

back to the anti-crossing point, and the two paths can coherently interfere. Putting things together, the LZS interferometry can be treated as a successive unitary transformation between the initial state and the final state as follows[32]:

$$|\Psi(\tau)\rangle = U_{(\tau,t_2)} U_{\mathrm{LZ}}^{T} U_{(t_2,t_1)} U_{\mathrm{LZ}} U_{(t_1,0)} |\Psi_{+}(0)\rangle, \tag{3}$$

where U is the evolution matrix for each segment and T denotes a transposition of the matrix (the explicit expressions are provided in the Supplementary Information).

Typically, not every closed loop in the parameter space can result in a cyclic evolution in the Hilbert space of the LZS interferometry. The experiment is equivalent to an optical interferometer, where we have the interference of paths in phase space rather than in coordinate space. The interference phase[33,35]

$$\Delta\varphi = \frac{1}{\hbar}\int_{t_1}^{t_2} [E_{-}(t) - E_{+}(t)]\, dt + 2\varphi_s, \tag{4}$$

depends on the magnitude of the qubit energy detuning excursion for times $t_1 < t < t_2$ (shaded region in Fig. 2b), φ_s is the Stokes phase. The destructive interference corresponds to integer values of $\Delta\varphi/2\pi$[33,35]. The destructive interference between the two transition paths, one through $|\Psi_{+}(t)\rangle$ and the other through $|\Psi_{-}(t)\rangle$ in the intermediate state, completely suppresses the probability to reach $|\Psi_{-}(t)\rangle$ after the second crossing. Therefore the system undergoes an evolution of returning to the initial state, $|\Psi_{+}(\tau)\rangle = \exp(i\varphi)|\Psi_{+}(0)\rangle$, and this cyclic evolution loop corresponds to the operation $U_{(\tau,0)}$ or $U(\theta, \varphi)$ in the basis states $|0\rangle$ and $|1\rangle$.

Different gates $U(\theta, \varphi)$ are achieved by adjusting the values of control parameters $\varepsilon_0(t)$, A and τ to satisfy the condition of destructive interference. The corresponding rotation angles of the gate operations are given by

$$\theta = \arctan\left(\frac{\Delta}{\varepsilon_0(0)}\right), \ \varphi = \varphi^d + \varphi^g, \tag{5}$$

the dynamical phase $\varphi^d = -\frac{1}{\hbar}\int_0^\tau \langle\Psi(t)|H(t)|\Psi(t)\rangle dt$; and an interpretation of the cyclic dynamics of the system is visualized in Fig. 2c, in which the value of the geometric phase φ^g corresponds to half of the solid angle swept by the state vector on the Bloch sphere[13,39,53] (see Supplementary Information for details on calculation of the dynamical and geometric phase). For examples, we evolve the pulse profiles $\varepsilon_0(t)$ along three different loops, with the parameters $(\varepsilon_0(t), A, \tau)$ chosen respectively as $(-45.2\,\mu\mathrm{eV}, 70.9\,\mu\mathrm{eV}, 257\ \mathrm{ps})$, $(-18.7\,\mu\mathrm{eV}, 27.2\,\mu\mathrm{eV}, 347\ \mathrm{ps})$, and $(-10.8\,\mu\mathrm{eV}, 15.4\,\mu\mathrm{eV}, 371\ \mathrm{ps})$. The three gates results from these cyclic evolutions are denoted by $U\left(\theta = \frac{\pi}{8}, \varphi = -\frac{3\pi}{2}\right)$, $U\left(\theta = \frac{\pi}{4}, \varphi = -\frac{3\pi}{2}\right)$, and $U\left(\theta = \frac{\pi}{3}, \varphi = -\frac{3\pi}{2}\right)$. The performance of the gates for three typical transformations is characterized by measured state tomography in Fig. 3.

Dephasing during the geometric LZS process. The experimentally obtained fidelity F of the gate process $U(\theta, \varphi)$ is provided in Fig. 4 as a function of total phase φ, with $\theta = 0$. The fidelity is defined as the overlap between the physical and ideal density matrices after the gate operations (see Supplementary Information for theoretical calculations of the fidelity). One can also capture the essence of the observations through the intuitive picture presented in the following. Generally, fluctuations from control field cause errors in the acquired phase $\varphi = \varphi^d + \varphi^g$ of the qubit. On one hand, if the fluctuations are sufficiently fast, the error in the geometric phase

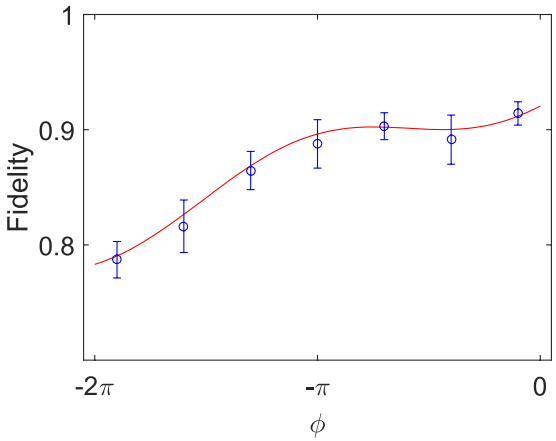

Figure 4. The fidelity *F* (blue circles) for the gates $U(\theta, \phi)$, are provided as a function of the total phase ϕ, with $\theta = 0$. The fidelity is estimated from the state tomography of the final states. The red line corresponds to the theoretically calculated fidelity including the noise effect.

φ^g is minimum since the solid angle of the loop is preserved on average[15,18,20,42,44,53]. However, in our experiment, there is low-frequency fluctuations in the control field $\varepsilon_0(t) + \delta\varepsilon_0$ induced by charge noise coupling to the qubit[48,50]. Thus, the geometric phase φ^g is sensitive to slow fluctuations, which cause the solid angle subtended by the path at the origin to change from one measurement to the next[18,44,53]. On the other hand, the dynamical phase φ^d is dominated by $\Delta\phi$ giving rise to the interference which is proportional to the duration of the accumulation process multiplied by the amplitude of the energy between two Landau-Zener tunneling points. The presence of the fluctuation field $\delta\varepsilon_0$ can change the position of the avoided level crossing and therefore cause fluctuations in φ^d[54]. In the future, the influence of the geometric and LZS component on the quantum gates can be utilized and distinguished in a systematic way by using spin-echo technique to remove the dynamical phase[15,39].

Discussion

In summary, we realize a geometric LZS interferometry on a semiconducting quantum dot qubit using well-designed electric control pulse. We can achieve non-adiabatic gate operations that correspond to a representation of the complete SU(2) group, which is a central ingredient in geometric quantum computation. We can also investigate the fidelity of the resulting gate operations in the presence of realistic decoherence. Moreover, universal gates with inherent fault-tolerant geometric features demonstrated for semiconducting quantum devices can be implemented in general physical systems.

Methods

The experiment was performed on a GaAs/AlGaAs heterostructure using a molecular-beam epitaxy, with a 95 nm deep two-dimensional electron gas (2DEG) with an electron density of 2.0×10^{11} cm^{-2} and a mobility of 6.0×10^4 cm^{-2}V^{-1}s^{-1} at 4 K. The metallic (Ti-Au) surface gates were fabricated using electron-beam lithography. Figure 2a provides the scanning electron micrograph of the surface gates which shape the double quantum dot and a nearby quantum point contact (QPC) charge-sensing channel.

The device was cooled inside an Oxford Triton dilution refrigerator to a base temperature of 30 mK. To reduce charge noise, the sample was cooled while a positive voltage bias was applied to all the gates. The plunge gate was connected to the bias-tees, which enabled the application of DC as well as high frequency control voltage to this gate.

As a result of the capacitive coupling between the dot and the sensing quantum point contact (QPC), the record current through the QPC is increased or decreased when an electron moves from the left dot to the right or vice versa. Thus, the conductance change through the QPC with and without the manipulation pulse is used to determine the average charge occupation and converted to the reported probabilities[48,49]. Our experiments are performed for a number of different runs. Since they have shown identical results and physics, we present, for consistency, only the data collected from one run.

References

1. Nielsen, M. A. & Chuang, I. L. *Quantum Computation and Quantum Information* (Cambridge Univ. Press, 2000).
2. Knill, E. Quantum computing with realistically noisy devices. *Nature* **434,** 39–44 (2005).
3. Raussendorf, R. & Harrington, J. Fault-tolerant quantum computation with high threshold in two dimensions. *Phys. Rev. Lett.* **98,** 190504 (2007).
4. Barrett, S. D. & Stace, T. M. Fault tolerant quantum computation with very high threshold for loss errors. *Phys. Rev. Lett.* **105,** 200502 (2010).
5. Wang, D. S., Austin, A. G. & Hollenberg, L. C. L. Quantum computing with nearest neighbor interactions and error rates over 1%. *Phys. Rev. A* **83,** 020302(R) (2011).
6. Buluta, I., Ashhab, S. & Nori, F. Natural and artificial atoms for quantum computation. *Rep. Progr. Phys.* **74,** 104401 (2011).
7. Benhelm, J., Kirchmair, G., Roos, C. F. & Blatt, R. Towards fault-tolerant quantum computing with trapped ions. *Nat. Phys.* **4,** 463–466 (2008).

8. Harty, T. P. *et al.* High-fidelity preparation, gates, memory, and readout of a Trapped-Ion Quantum Bit. *Phys. Rev. Lett.* **113,** 220501 (2014).
9. Barends, R. *et al.* Superconducting quantum circuits at the surface code threshold for fault tolerance. *Nature* **508,** 500–503 (2014).
10. Bluhm, H. *et al.* A. Dephasing time of GaAs electron-spin qubits coupled to a nuclear bath exceeding 200 μs. *Nat. Phys.* **7,** 109 (2011).
11. Forster, F. *et al.* Characterization of qubit dephasing by Landau-Zener-Stückelberg-Majorana interferometry. *Phys. Rev. Lett.* **112,** 116803 (2014).
12. Berry, M. V. Quantal phase-factors accompanying adiabatic changes. *Proc. R. Soc. Lond. A* **392,** 45–57 (1984).
13. Aharonov, Y. & Anandan, J. Phase-change during a cyclic quantum evolution. *Phys. Rev. Lett.* **58,** 1593–1596 (1987).
14. Wilczek, F. & Zee, A. Appearance of gauge structure in simple dynamical systems. *Phys. Rev. Lett.* **52,** 2111–2114 (1984).
15. Sjöqvist, E. A new phase in quantum computation. *Physics* **1,** 35 (2008).
16. Jones, J. A., Vedral, V., Ekert, A. & Castagnoli, G. Geometric quantum computation using nuclear magnetic resonance. *Nature* **403,** 869–871 (2000).
17. Leibfried, D. *et al.* Experimental demonstration of a robust, high-fidelity geometric two ion-qubit phase gate. *Nature* **422,** 412–415 (2003).
18. Leek, P. J. *et al.* Observation of Berry's phase in a solid-state qubit. *Science* **318,** 1889–1892 (2007).
19. Mottonen, M., Vartiainen, J. J. & Pekola, J. P. Experimental determination of the Berry phase in a superconducting charge pump. *Phys. Rev. Lett.* **100,** 177201 (2008).
20. Filipp, S. *et al.* Experimental demonstration of the stability of Berry's phase for a spin-1/2 particle. *Phys. Rev. Lett.* **102,** 030404 (2009).
21. Wu, H. *et al.* Geometric phase gates with adiabatic control in electron spin resonance. *Phys. Rev. A* **87,** 032326 (2013).
22. Zanardi, P. & Rasetti, M. Holonomic quantum computation. *Phys. Lett. A* **264,** 94–99 (1999).
23. Duan, L. M., Cirac, J. I. & Zoller, P. Geometric manipulation of trapped ions for quantum computation. *Science* **292,** 1695–1697 (2001).
24. Solinas, P., Zanardi, P., Zanghi, N. & Rossi, F. Holonomic quantum gates: a semiconductor-based implementation. *Phys. Rev. A* **67,** 062315 (2003).
25. Faoro, L., Siewert, J. & Fazio, R. Non-abelian holonomies, charge pumping, and quantum computation with Josephson junctions. *Phys. Rev. Lett.* **90,** 028301 (2003).
26. Kamleitner, I., Solinas, P., Muller, C., Shnirman, A. & Mottonen, M. Geometric quantum gates with superconducting qubits. *Phys. Rev. B* **83,** 214518 (2011).
27. Sjoqvist, E., Tong, D. M., Hessmo, B., Johansson, M. & Singh, K. Non-adiabatic holonomic quantum computation. *N. J. Phys.* **14,** 103035 (2012).
28. Abdumalikov Jr, A. A. *et al.* Experimental realization of non-Abelian non-adiabatic geometric gates. *Nature* **496,** 482–485 (2013).
29. Feng, G., Xu, G. & Long, G. Experimental realization of nonadiabatic holonomic quantum computation. *Phys. Rev. Lett.* **110,** 190501 (2013).
30. Arroyo-Camejo, S., Lazariev, A., Hell, S. W. & Balasubramanian, G. Room temperature high-fidelity holonomic single-qubit gate on a solid-state spin. *Nat. Commun.* **5,** 4870 (2014).
31. Zu, C. *et al.* Experimental realization of universal geometric quantum gates with solid-state spins. *Nature* **514,** 72 (2014).
32. Shevchenko, S. N. *et al.* Landau-Zener-Stückerlberg Interferometry. *Phys. Rep.* **492,** 1–30 (2010).
33. Oliver, W. D. *et al.* Mach-Zehnder interferometry in a strongly driven superconducting qubit. *Science* **310,** 1653–1657 (2005).
34. Sillanpaa, M., Lehtinen, T., Paila, A., Makhlin, Y. & Hakonen, P. Continuous-time monitoring of Landau-Zener interference in a Cooper-pair box. *Phys. Rev. Lett.* **96,** 187002 (2006).
35. Petta, J. R., Lu, H. & Gossard, A. C. A coherent beam splitter for electronic spin states. *Science* **327,** 669–672 (2010).
36. Gasparinetti, S., Solinas, P. & Pekola, J. P. Geometric Landau-Zener interferometry. *Phys. Rev. Lett.* **107,** 207002 (2011).
37. Tan, X. S. *et al.* Demonstration of geometric Landau-Zener interferometry in a superconducting qubit. *Phys. Rev. Lett.* **112,** 027001 (2014).
38. Zhang, J., Zhang, J., Zhang, X. & Kim, K. Realization of geometric Landau-Zener-Stückelberg interferometry. *Phys. Rev. A* **89,** 013608 (2014).
39. Zhu, S. L. & Wang, Z. D. Implementation of universal quantum gates based on nonadiabatic geometric phases. *Phys. Rev. Lett.* **89,** 097902 (2002).
40. Zhu, S. L. & P. Zanardi. Geometric quantum gates that are robust against stochastic control errors. *Phys. Rev. A* **72,** 020301(R) (2005).
41. Carollo, A., Fuentes-Guridi, I., Santos, M. F. & Vedral, V. Geometric phase in open systems. *Phys. Rev. Lett.* **90,** 160402 (2003).
42. De Chiara, G. & Palma, G. M. Berry phase for spin 1/2 particle in a classical fluctuating field. *Phys. Rev. Lett.* **91,** 090404 (2003).
43. Blais, A. & Tremblay, A. M. S. Effect of noise on geometric logic gates for quantum computation. *Phys. Rev. A* **67,** 012308 (2003).
44. Solinas, P., Zanardi, P. & Zanghi, N. Robustness of non-Abelian holonomic quantum gates against parametric noise. *Phys. Rev. A* **70,** 042316 (2004).
45. Tong, D. M., Sjoqvist, E., Kwek, L. C. & Oh, C. H. Kinematic approach to the mixed state geometric phase in nonunitary evolution. *Phys. Rev. Lett.* **93,** 080405 (2004).
46. Oreshkov, O., Brun, T. A. & Lidar, D. A. Fault-tolerant holonomic quantum computation. *Phys. Rev. Lett.* **102,** 070502 (2009).
47. Thomas, J. T., Lababidi, M. & Tian, M. Z. Robustness of single-qubit geometric gate against systematic error. *Phys. Rev. A* **84,** 042335 (2011).
48. Cao, G. *et al.* Ultrafast universal quantum control of a quantum-dot charge qubit using Landau-Zener-Stückelberg interferometry. *Nat. Commun.* **3,** 1401 (2013).
49. Hanson, R., Kouwenhoven, L. P., Petta, J. R., Tarucha, S. & Vandersypen, L. M. K. Spins in few-electron quantum dots, *Rev. Mod. Phys.* **79,** 1217–1265 (2007).
50. Petersson, K. D., Petta, J. R., Lu, H. & Gossard, A. C. Quantum coherence in a one-electron semiconductor charge qubit. *Phys. Rev. Lett.* **105,** 246804 (2010).
51. Hayashi, T., Fujisawa, T., Cheong, H. D., Jeong, Y. H. & Hirayama, Y. Coherent manipulation of electronic states in a double quantum dot. *Phys. Rev. Lett.* **91,** 226804 (2003).
52. Zhu, S. L. & Wang, Z. D. Universal quantum gates based on a pair of orthogonal cyclic states: Application to NMR systems. *Phys. Rev. A* **67,** 022319 (2003).
53. Berger, S. *et al.* Exploring the effect of noise on the Berry phase. *Phys. Rev. A* **87,** 060303(R) (2013).
54. Huang, P. *et al.* Landau-Zener-Stückelberg interferometry of a aingle electronic spin in a noisy environment. *Phys. Rev. X* **1,** 011003 (2011).

Acknowledgements

This work was supported by the National Fundamental Research Program (Grant No. 2011CBA00206), and the National Natural Science Foundation (Grant Nos. 11274294, 11474270).

Author Contributions

T.T., L.W. and G.C.G. designed the experiment, provided theoretical support and analyzed the data. L.W., B.G. and C.Z. fabricated the samples and performed the measurements.

Additional Information

Supplementary information accompanies this paper at http://www.nature.com/srep

Competing financial interests: The authors declare no competing financial interests.

How to cite this article: Wang, L. *et al.* Experimental realization of non-adiabatic universal quantum gates using geometric Landau-Zener-Stückelberg interferometry. *Sci. Rep.* **6**, 19048; doi: 10.1038/srep19048 (2016).